

Full Paper

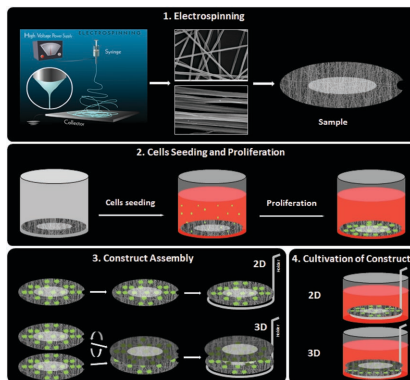
Differentiation of Human Mesenchymal Stem Cells Toward Quality Cartilage Using Fibrinogen-Based Nanofibers

J. Forget, F. Awaja, D. Gugutkov, J. Gustavsson, G. Gallego Ferrer, T. Coelho-Sampaio, C. Hochman-Mendez, M. Salmeron-Sánchez, G. Altankov*

Macromol. Biosci. **2016**, *xx*, 000–000




Early View Publication; these are NOT the final page numbers, use DOI for citation !!

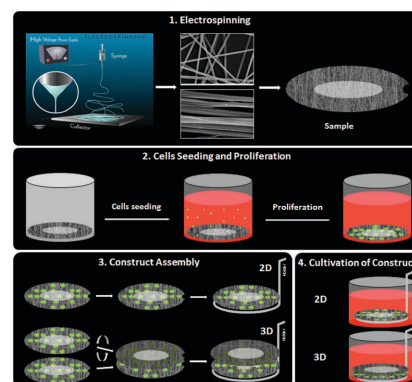




The illustration of the preparation steps for the 2D and 3D constructs, including: (1) production of samples via deposition of random or aligned electrospun nanofibers on gel slices, (2) seeding of ADSCs and their propagation up to confluency, (3) assembly of the constructs, either in 2D (single slides) or 3D (sandwich-like) configuration, and (4) cultivation of living construct in chondrogenic differentiation medium.

Differentiation of Human Mesenchymal Stem Cells Toward Quality Cartilage Using Fibrinogen-Based Nanofibers

J. Forget, F. Awaja, D. Gugutkov,  Gustavsson, G. Gallego Ferrer, T. Coelho-Sampaio, C. Hochman-Mendez, M. Salmeron-Sánchez, G. Altankov*

Mimicking the complex intricacies of the extra cellular matrix including 3D configurations and aligned fibrous structures were traditionally perused for producing cartilage tissue from stem cells. This study shows that human adipose derived mesenchymal stem cells (hADMSCs) establishes significant chondrogenic differentiation and may generate quality cartilage when cultured on 2D and randomly oriented fibrinogen/poly-lactic acid nanofibers compared to 3D sandwich-like environments. The adhering cells show well-developed focal adhesion complexes and actin cytoskeleton arrangements confirming the proper cellular interaction with either random or aligned nanofibers. However, quantitative reverse transcription-polymerase chain reaction analysis for Collagen 2 and Collagen 10 genes expression confirms favorable chondrogenic response of hADMSCs on random nanofibers and shows substantially higher efficacy of their differentiation in 2D configuration versus 3D constructs. These findings introduce a new direction for cartilage tissue engineering through providing a simple platform for the routine generation of transplantable stem cells derived articular cartilage replacement that might improve joint function.



J. Forget
BioElpida
Lyon, France
F. Awaja, D. Gugutkov,  Gustavsson,
T. Coelho-Sampaio, G. Altankov
Institute for Bioengineering of Catalonia (IBEC)
Barcelona, Spain
E-mail: george.altankov@icrea.cat
G. Gallego Ferrer
Center for Biomaterials and Tissue Engineering (CBIT)
Universitat Politècnica de València
Valencia, Spain
G. Gallego Ferrer, G. Altankov 
Biomedical Research Network Center in Bioengineering
Biomaterials and Nanomedicine (CIBER-BBN)
Spain

T. Coelho-Sampaio, C. Hochman-Mendez
Federal University of Rio de Janeiro
Brazil
M. Salmeron-Sánchez
Division of Biomedical Engineering
School of Engineering
University of Glasgow
Glasgow G12 8LT, UK
G. Altankov
Institutio Catalana de Recerca i Estudis Avançats (ICREA)
Barcelona, Spain



1. Introduction

Musculoskeletal disorders caused by aging, trauma, or osteoarthritis commonly result in a degeneration of the hyaline cartilage. Postnatal cartilage however lacks the ability to self-repair completely through native healing mechanisms^[1] because the chondrocytes are embedded in a dense layer of extra cellular matrix (ECM) which hampers their mobility.^[2] In addition, articular surface is avascular which further limits its capacity to regenerate.^[3] Traditionally, temporary solutions have been used for resolving early to middle stage osteoarthritis cases by using multiple surgical techniques like micro fracture, mosaicplasty, osteochondral allograft transplantation, etc., with limited success.^[4,5] Engineering artificial cartilage is promising, although inconsistent so far, to provide permanent replacement of damaged tissue^[1–3,6–8] avoiding heavy reconstructive surgery.^[1,6,9,10]

Most of the ECM fibrils within tissues are not random and exhibit well defined patterns and specific spatial orientation. Therefore, it is anticipated that the geometry of cellular interaction within a scaffold is a key parameter in cartilage tissue engineering and should mimic to a great extent the natural organization of ECM fibrils.^[11] Indeed, distinct organizational features are strongly influential in directing cell behavior. For example, Xu et al.^[12] show that both adhesion and proliferation of smooth muscle cells are improved on oriented nanofibrous scaffolds. However the data for other cell types including chondrocytes are rather sparse and controversial.^[13,14] Recent findings demonstrated that oriented nanofibrous scaffolds have the potential for engineering blood vessels,^[12] neural tissue,^[15] and ligaments,^[16] for cartilage, however, such studies are rather missing or incomplete.^[17–19]

Another important issue is the source of the cells that might promise proper cartilage repair. Vacanti's research group successfully produced hyaline-like tissue from adult bovine chondrocytes using polylactic-polyglycolic acid matrices.^[20,21] The use of both autogenous and allograft chondrocytes for engineering cartilage, however, is problematic because of a relatively small cellular yield at harvest, thereby imposing long culture expansion while cells tend to de-differentiate.^[22] Alternatively, multiple reports such as that of Bruder et al.^[23] engineered bone and cartilage using mesenchymal stem cells derived from bone marrow.^[24] Harvesting of these cells, however, is painful with limited yields (<0.1%), especially in the elder patients, again making culture expansion necessary.^[25]

This present study is focused on producing a quality cartilage based on a specifically engineered nanofibers scaffold able to support differentiation of stem cells where the role of both nanofibers orientation (random vs aligned) and dimensionality (2D vs 3D environment) are clearly addressed. Human adipose derived mesenchymal

stem cells (hADMSCs) were used as cell model considering easy adaptation for biomedical application. These stem cells are easier to obtain, show lower donor site morbidity, are available in larger numbers,^[25] and have at least a trilineage potential to form bone, cartilage, and fat.^[26] To engineer the scaffold we used electro-spun hybrid fibrinogen/polylactic acid (FBG/PLA) nanofibers recently developed in our laboratory. Those nanofibers have well-tuned mechanical properties that allow for the arrangement of both 2D and 3D (sandwich-like) constructs and preserve the excellent cell recognition property of native FBG.^[27]

Using a combination of our innovative technology and established protocols,^[27–30] we obtained fibers with an average diameter of 382 ± 120 nm for random samples and of 298 ± 96 for aligned ones ($n = 100$). These values are in good agreement with previously reported values for other composite fibrinogen nanofibers, varying between 140 and 640 nm for PLA/PCL/fibrinogen nanofibers^[30] depending on the polymer ratio (20–100%, v/v).

The processing step of the production of FBG/PLA nanofibers by electrospinning is illustrated in Figure 1.1. A mixture of FBG and PLA in hexafluoroisopropanol (HFIP) was electrospun as a homogenous layer of either random or aligned fibers. In the case of the aligned nanofibers, the pixel intensity distribution obtained from Fast Fourier transformation (FFT) analyses of representative scanning electron microscope (SEM) images revealed that the majority of the fibers align within 10° of the common fiber direction (Figure 2). The mechanical properties of dry nanofibers were determined by AFM. Figure 3 shows that the reinforcement of FBG nanofibers with PLA substantially increased the local stiffness of the fibers from 30 ± 10 to 275 ± 50 Nm^{-1} . Meanwhile, pure PLA fibers were significantly stiffer than composite nanofibers (4000 ± 400 Nm^{-1}).

Initial cellular response to a ventral contact with composite nanofibers was evaluated morphologically in a short-term culture conditions. After 2 h of incubation in a serum free medium, to avoid the effect of other serum proteins, adhesion to random nanofibers promoted an irregular cell shape with multiple cytoplasmic projections extending toward differently oriented fibers (Figure 4a and c).

The cell protrusions showed high accumulation of actin that co-localized with vinculin in focal adhesions (Figure 4c) suggesting firm adhesive interaction with fibers. On the other hand, the cells adhering to the aligned fibers (Figure 4b and d) showed an elongated morphology that strongly follows the fiber's orientation. The highly extended actin stress fibers entering into well-developed focal adhesion complexes (Figure 4d) again indicate a firm cell-substratum interaction.

Early passage human ADSCs were first seeded onto random or aligned nanofibers in 2D configuration



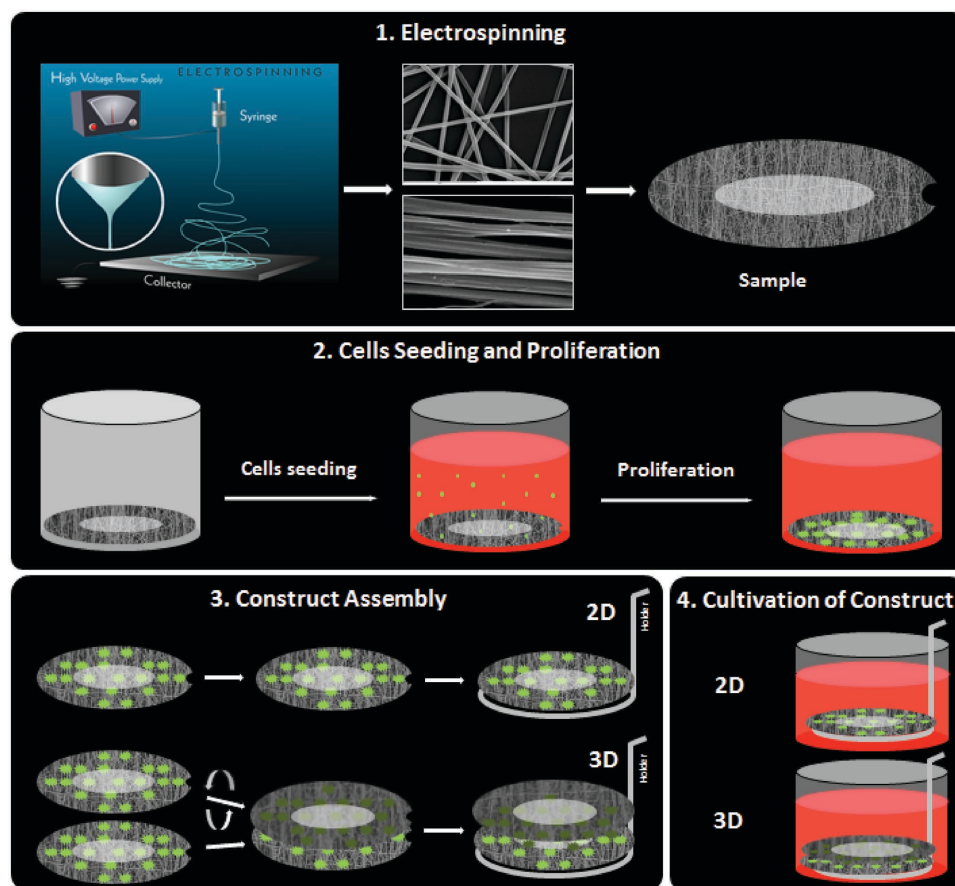


Figure 1. Scheme illustrating the main steps for the preparation of 2D and 3D constructs, involving: 1) production of samples via deposition of random or aligned electrospun nanofibers on gel slices, 2) seeding of ADSCs and their propagation up to confluency, 3) assembly of the constructs, either in 2D (single slides) or 3D (sandwich-like) configuration, and 4) cultivation of living construct in chondrogenic differentiation medium.

(Figure 1.1) and cultured for 3–5 d upon rich confluence (Figure 1.2) before being switched to chondrogenic differentiation conditions under 2D or 3D environment (Figure 1.3) and culture up to 50 d (Figure 1.4).

As shown on Figure 1.3, for the differentiation of cells in 2D environment, the constructs were simply switched to complete Chondrogenic medium and cultured for 50 d. For the creation of 3D environment, a sandwich-like constructs were assembled by joining two cell-loaded constructs, random or aligned, to face each other with their cellular sites.

To confirm cells viability at this stage (before assembly of the constructs), some samples were stained with fluorescein diacetate (FDA). Representative pictures are shown in Figure 5 demonstrating abundant green staining of viable cells that indicate the successful conversion of FDA to its fluorescent analogue. Both 2D and 3D constructs were further cultured for 50 d in cartilage inducing conditions resulting in the appearance of glossy cartilage like tissue (Figure 6), particularly for 2D samples, that were clearly Safranin Red positive (bottom right).

Overall, visual inspection of the cartilage tissue indicated better formation and homogeneity in 2D environment, particularly on random samples (lower panel), while on 3D constructs, the cartilage tissue tends to detach from the supporting hydrogel holders and often roll up over the surface when the two holders were separated (Figure 6 upper panel).

Cartilage tissue that was generated using the 2D configuration for both aligned and random fibers were further stained for actin and nuclei and subjected to a confocal microscopy to examine the overall organization and homogeneity of cell layers. It was not feasible to investigate the cartilage tissue produced with the 3D construct samples because of the tendency for sequestration of both layers. As shown on Figure 7 the cell distribution was more homogenous in random nanofibers samples compared to the aligned ones, where the cells crowding results in a rather island-like aggregates.

Vertical reconstruction of the confocal images shows that the majority of the cells do not penetrate within the scaffold but tend to make a monolayer over the surface,

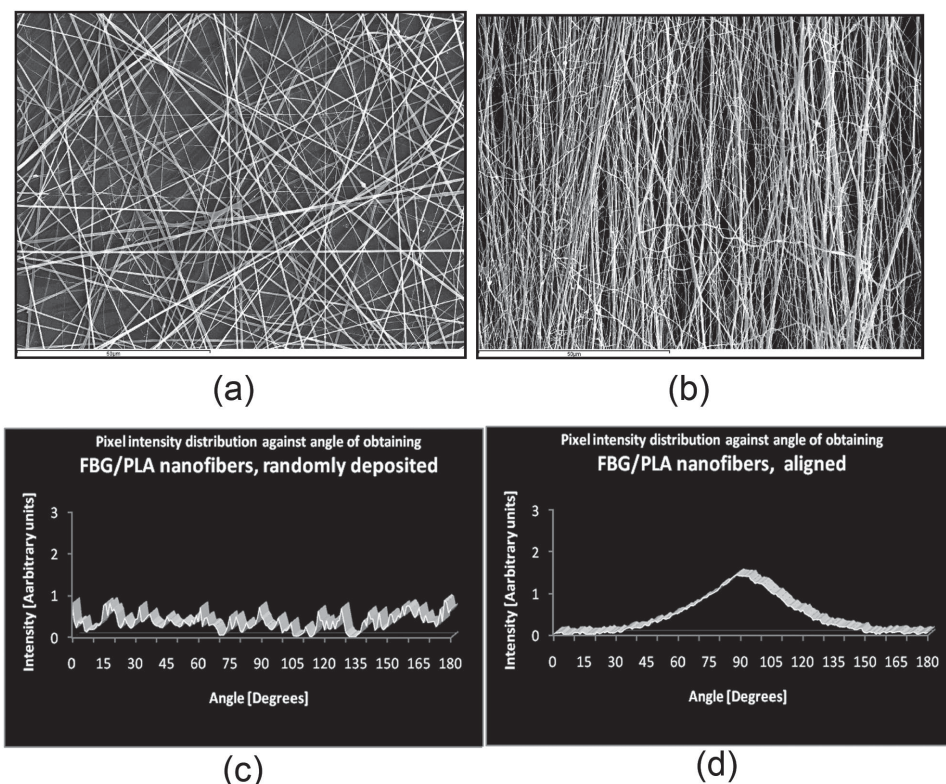


Figure 2. SEM images of the a) random and b) aligned FBG/PLA nanofibers and the respective pixel intensity distribution for the c) random and d) aligned samples.

which is more homogenous for random nanofiber samples and with a tendency for clustering at aligned nanofiber configuration.

Regarding the morphological response of the adhering stem cells, it is well documented that the cells display a variety of shapes depending on the geometry of adhesive environment on which they adapt their cytoskeleton.^[31] Indeed, the presence of highly extended actin stress fibers in aligned samples that penetrate into focal adhesions indicates that ADSCs apply significant traction over

the FBG-PLA fibers thus acquiring strongly elongated morphology. Conversely, the overall shape of cells on random fibers resembles, to a large extent, the stellate-like morphology characteristic for cells residing in 3D environment.^[32] We found, previously, similar morphological response of endothelial cells culturing on the present composite FBG/PLA nanofibers (not shown here), or on pure FBG nanofibers.^[27] Considering however that the cells cannot enter between fibers, even at longer incubations, evident from the reconstructed confocal images in Figure 7,

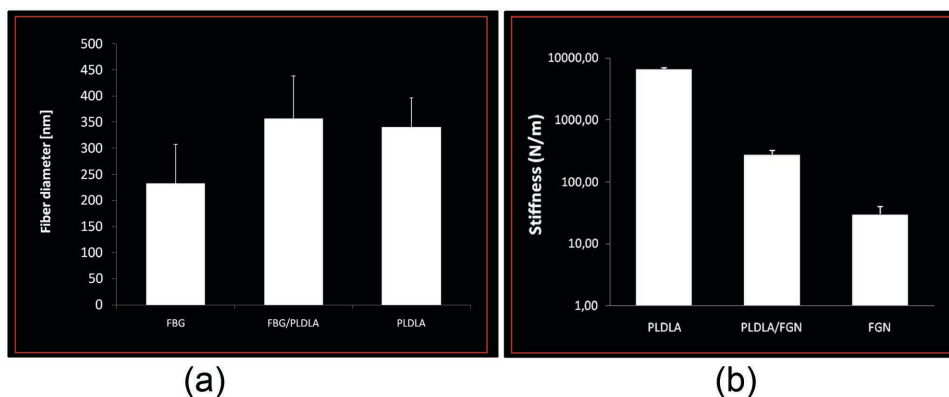


Figure 3. Comparison of fiber's a) diameter and b) stiffness between plain FBG and PLDL nanofibers, and the composite PLDLA/FBG nanofibers.

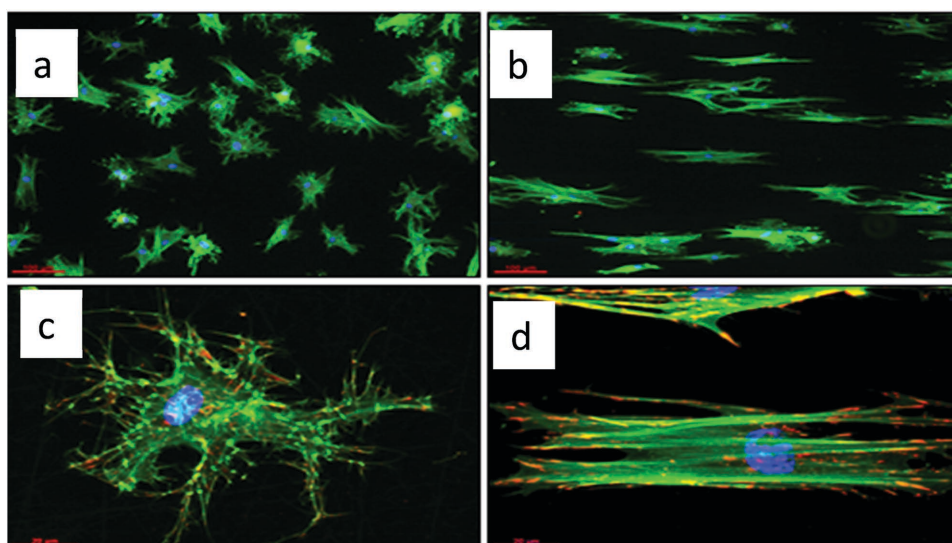


Figure 4. Overall morphology of ADSCs on a,c) random and b,d) aligned FBG/PLA nanofibers viewed at different magnifications. The adhering cells on the aligned nanofibers represent typically extended shapes that strongly follow the fiber's orientation, while on random nanofibers they spread in multiple directions and develop stellate-like morphology.

and somewhat overlay them, we concluded that though the cells sense fibers rather as topography (i.e., 2.5 D) they clearly respond to their organization.

To measure and compare the thickness of the resulting cartilage, small tissue disks were obtained from the middle part of the samples and cut transversally (see Section 3) to be examined microscopically. As shown in Figure 8 the thickness of the cartilage tissue vary significantly between the random (bottom panel) and aligned (upper panel) samples.

Upon visual inspection, the cartilage tissue that is generated from the aligned nanofibers was friable. In 3D constructs it appeared relatively thick, about 420 μm , but tended to split and separate when recovering the sample from the two layers. The thickness of the 3D aligned constructs varied significantly, between 181–536 μm , confirming their inhomogeneity

seen on confocal images. On the other hand, the cartilage tissue in 2D samples showed a thickness values between 152 and 161 μm and without significant variations in homogeneity. Overall, the cartilage tissue in 2D random samples looks more compact and dense with pronounced follicular morphology under phase contrast reminiscent for native cartilage.^[33] In Figure 9, which characterize the overall deposition of glycoaminoglycans viewed by Alcian Blue staining, 2D random samples again show most compact organization with defined interface adjacent to the nanofibers layer (see arrow). In contrast, the 2D aligned samples show rather disorganized interface. Visibly less dye deposition was observed on 3D samples. Collagen type II matrix also show predominant accumulation in 2D aligned samples (Figure 10 left panels), while randomly aligned samples shows denser manifestation.

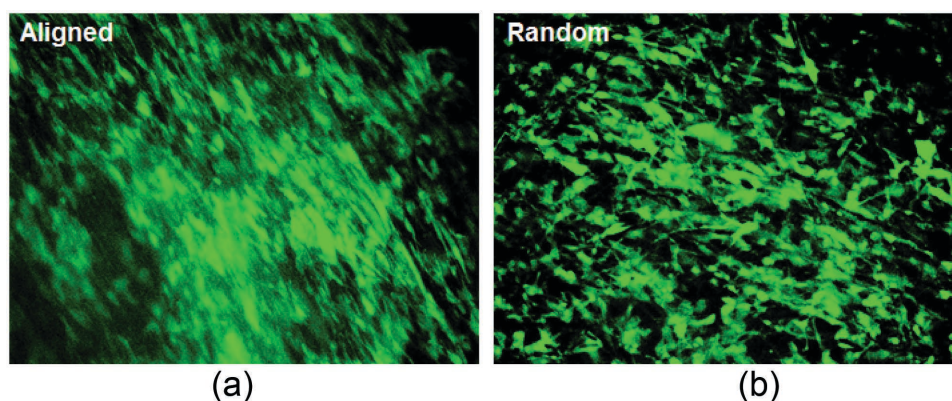


Figure 5. Viability of ADSCs cultured for 3 d on: a) aligned and b) random nanofibers. FDA demonstrates abundant conversion of the dye to its fluorescent analogue (green) confirming the viability of cells within the confluent layers (magnification 10 \times).

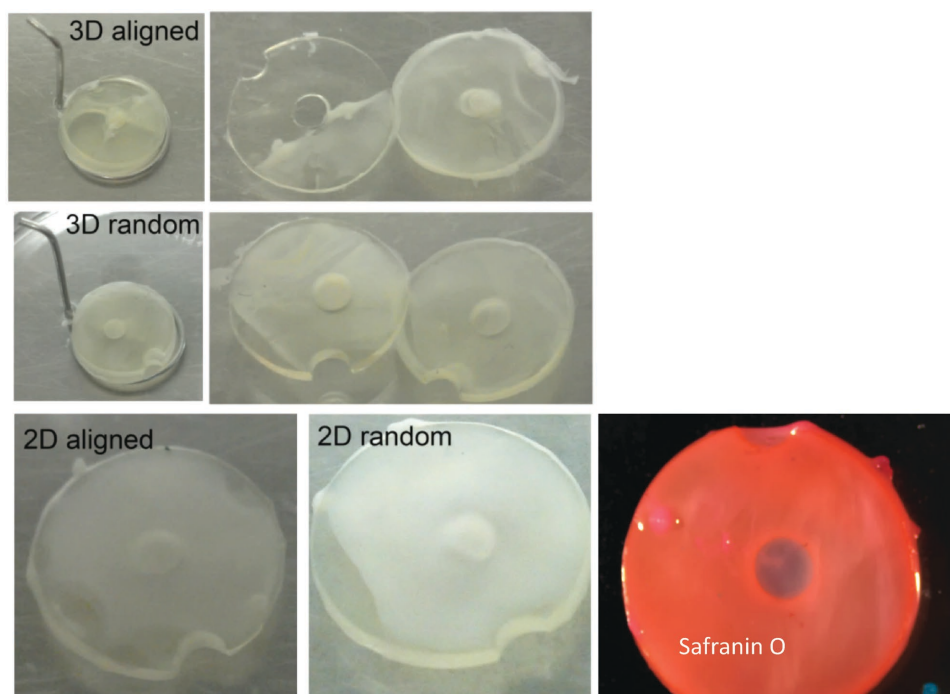


Figure 6. Cartilage production in vitro at 2D (lower row) and 3D (upper two rows) environment, in either random or aligned configurations, at 50th d of culture. Safranin O staining (right) confirms the cartilage-like nature of the resulting tissue.

Quantitative reverse transcription-polymerase chain reaction analysis for Collagen 2 and Collagen 10 genes expression confirmed favorable chondrogenic response of the hADMSCs on random nanofibers and showed substantially higher efficacy of their differentiation in 2D configuration versus 3D constructs. Quantitative RT PCR measurements shown in Figure 11 also confirmed the favorable chondrogenic response of hADMSCs in 2D environment. The chondrogenic markers, Col 2 and Col 10 were upregulated in all type of constructs even though the levels of upregulation were significantly different.

In general, they were very low expressed in non-activated ADSCs (cultured on basal medium) and moderately activated in pallet cultures. Both markers however were

better expressed in nanofibrous environment, particularly on 2D random nanofibers where Col 2 and Col 10 significantly override all other samples, including 3D random and all basic controls. A clear tendency for higher activity of Col 2 and Col 10 on 2D versus 3D constructs was observed also for aligned samples. Thus, our in vitro results show that the chondrogenic activity of ADSCs in most nanofibrous scaffolds significantly overrides those of the pallet cultures, which are the golden standard for in vitro cartilage production.^[34,35] They also suggest that Col 2 and Col 10 are promising candidates for genes that are strongly affected by nanofibers dimensionality and organization.

Hereby, we make an attempt at explaining the tendency of random nanofibers (on 2D construct) to favor

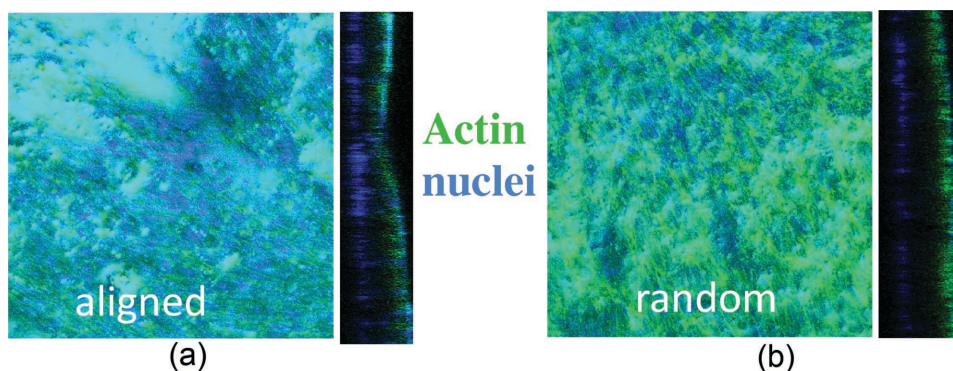


Figure 7. Confocal images in maximum projection mode showing the overall organization of cellular layers on a) aligned and b) random nanofibers samples cultured at 2D environment. Tangential reconstruction of the cell layers obtained from a Z-stack is shown on the right to each image.

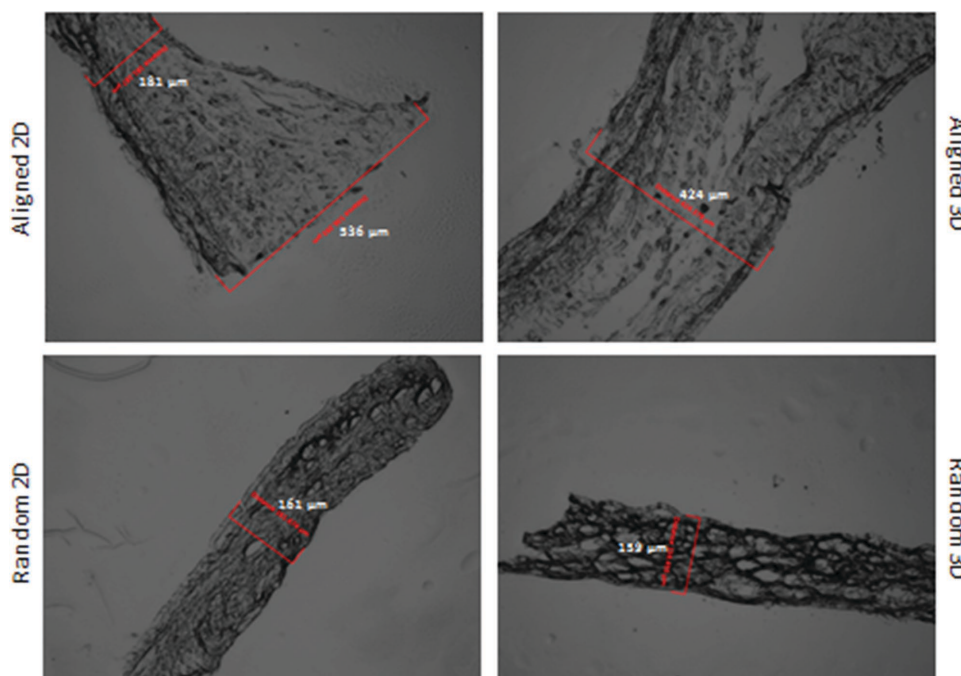


Figure 8. Morphology of the cartilage samples cultured in 2D and 3D environment in either random or aligned configuration cut transversally and viewed in optical microscope with phase contrast. The thickness of the samples is measured at the middle part of the constructs that contains only nanofibers.

stem cells differentiation since it contradicts earlier convention that oriented collagen fibrils are thought of as a catalyst for better superficial cartilage matrix.^[36] Compared to other zones of articular cartilage, the superficial zone consists of the highest concentration of tangentially oriented collagen fibrils, mainly type 2, and the lowest concentration of proteoglycans.^[37] This is obviously connected with the physiological ability of cartilage to withstand the tensile and compressive loading^[38] but is unrelated to optimal cellular interaction. Hence, our results are not in agreement with what the traditionally thought of in terms of having the aligned nanofibers to be better suited than random nanofibers for producing cartilage tissue in vitro.^[13,19,39]

Regarding the role of nanofibers dimensionality, our PCR data unexpectedly show a significantly higher cartilage specific gene activity in 2D environment versus the 3D environment, in agreement with the visual morphological inspection above for favored Collagen II and glycosaminoglycans deposition. We eliminated possible differences in medium or nutrition exposure of the two environments by measuring the activity of only middle part of construct. Hence, no reduction in medium exposure is foreseen, but it is probable that random nanofibers provoke the immobilization of stem cells, as we showed with other cell types^[27] and also for ADSCs (not shown here), which would support their differentiation—a situation that cannot be recapitulated in vivo.

Comparison between our results and previous research in the field showed agreements regarding the feasibility of cellular interaction with nanofibers. Li et al.^[40] have used electrospinning to obtain nanofibers composed of poly-caprolactone and showed their ability to maintain chondrocytes in a mature functional state. Further studies demonstrated that the maintenance of a chondrocytic phenotype is enhanced on nanofibers with dimensions similar to the native ECM, e.g., in the nano region, when compared to micro-sized fibers.^[41] A number of preceding studies, including ours, were focused on mimicking the fibrous protein structure of ECM utilizing different polymer-based fibrous scaffolds.^[42] Up to this point, pellet cultures—thought of as the golden standard in cartilage engineering^[35] was considered to work as positive control. Nevertheless, our nanofibers scaffolds strongly supersede the pellets in their ability to enhance chondrogenic differentiation of ADSCs thus confirming other studies indicating increased ECM production and cartilage specific gene expression on polymer fibrous scaffolds, while supporting cell proliferation.^[13,43]

Typically, organized fibrils within a scaffold are thought to promote cell migration and thus probably contribute to improving cartilage regeneration.^[13,39,44] Our previous studies with endothelial cells also support this view^[27] pointing on the regenerative potential of these cells at the vessel wall. The results presented here, however, on the differentiation of ADSCs to cartilage, are

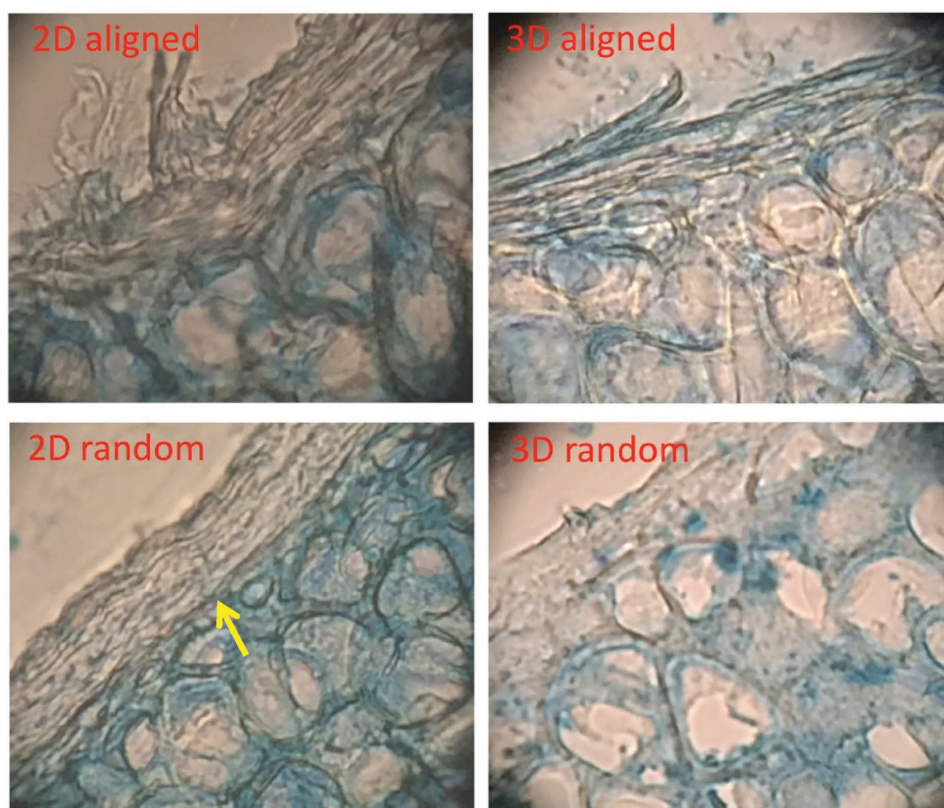


Figure 9. Morphology of the cartilage samples cultured in 2D and 3D environment in either random or aligned configuration stained to detect the presence of glycosaminoglycans by Alcian Blue staining. The slices derived from the center of the constructs, so the nanofibers were not in contact with the supporting gel. They were cut transversally and viewed in optical microscope. The scale bar corresponds to 100 μm and applies to the four panels.

contrary to typical observations. We generally found a better organized cartilage matrix on random nanofibers representing more homogenous structure in both, 2D or 3D environment as can be seen on Figures 7 and 8. In addition, the morphological appearance of this cartilage is reminiscent to the classical morphological view of rib cartilage sections when viewed by phase contrast microscopy.^[33] This trend was additionally confirmed by the quantitative PCR for Col 2 and Col 10 genes expression (Figure 9) indicating that temporary immobilization of stem cells is significant for acquiring chondrogenic phenotype.

Cartilage has a distinctive histology represented by chondrocytes surrounded by a homogeneous matrix composed of small parallel oriented collagen fibrils^[36] widely separated by aggregated structure of proteoglycan, hyaluronic acid, and link protein.^[44] In fact, this arrangement of collagen fibrils and space-filling proteoglycan aggregates generates a cushioning matrix that resists compression. This same cushioning matrix however as stated above is thought to be the reason for low regenerative potential of local chondrocytes blocking their migration in addition to the lack of nutrition due to missing vasculature. It is

noteworthy that both problems were eliminated in our in vitro system.

2. Conclusion

We have successfully produced cartilage using bioinspired nanofibers (containing natural FBG) at different configurations which show better quality and homogeneity in 2D than those produced in 3D environment. Moreover, nanofibers that were constructed in random configurations performed better than aligned nanofibers. This might serve as another illustration that an engineered device does not need to mimic exactly the natural environment but rather to follow its functional performance.

We further found that Col 2 and Col 10 are promising candidates for genes that are strongly affected by nanofibers dimensionality and organization. It should be further emphasized that in our conditions, the nanofibers organization affects ADSCs morphological response even in the absence of serum, obviously due to the contained fibrinogen, which is well-recognized by stem cells. This is a fact that has distinct value when one considers the

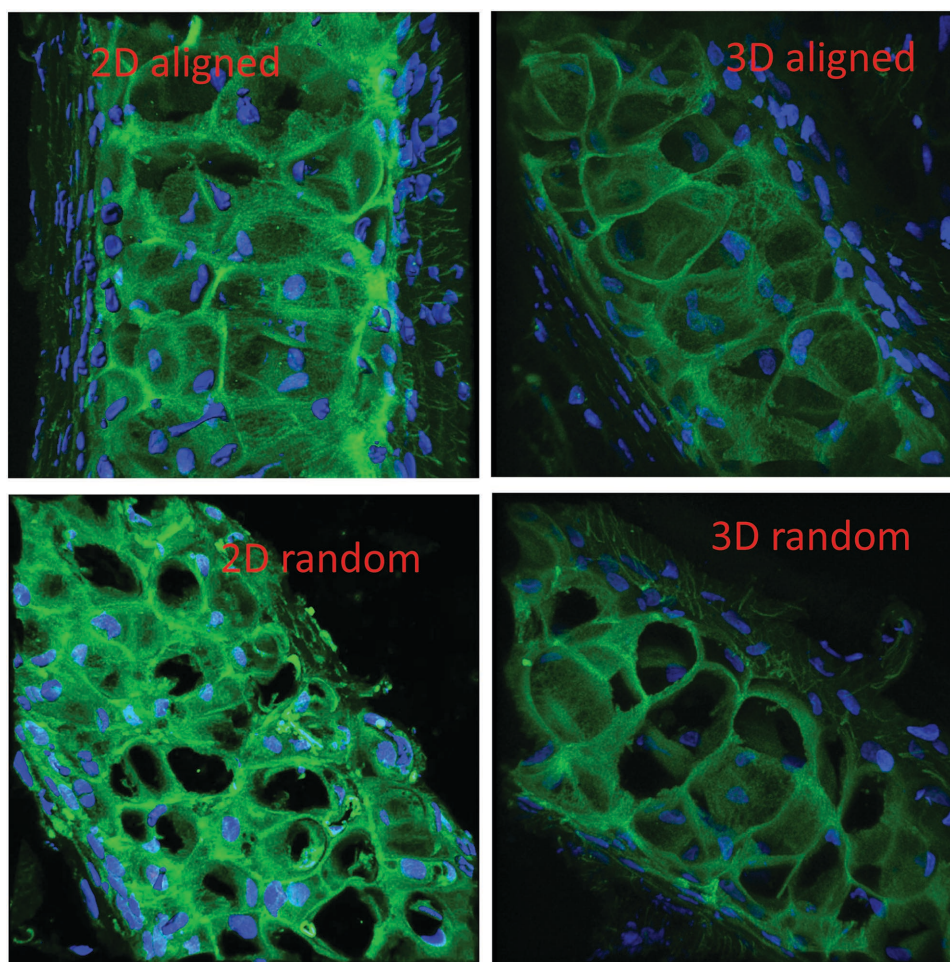


Figure 10. Morphology of the cartilage samples cultured in 2D and 3D environment in either random or aligned configuration stained to detect the presence of collagen II by immunofluorescence. The scale bar corresponds to 20 μm and applies to the four panels. Note the denser nature of the collagen II-stained matrix obtained on the 2D random constructs.

biomedical application of the proposed novel FBG/PLA nanofibers under GMP conditions.

3. Experimental Section

3.1. Electrospinning of FBG/PLA Nanofibers

For the production of FBG/PLA composite nanofibers, fibrinogen from bovine plasma (Sigma-Aldrich) and poly-L-DL-lactic acid 70:30 (PURAC) were separately dissolved in 1-1-1,3-3-3-HFIP (Sigma-Aldrich). Bovine fibrinogen (Sigma Aldrich, Spain) was freshly dissolved (100 mg mL^{-1}) in a 9:1 mixture of HFIP and $10\times$ DMEM (Invitrogen) and centrifuged at 4000 rpm for 10 min to remove insoluble precipitates. A conventional setup was used for electrospinning based on a high voltage supply (Glassman High Voltage Inc., USA) and a grounded collector. Randomly deposited nanofibers were obtained by vertical electrospinning onto gel-rings placed on aluminum foil. The applied voltage in both cases was 25–30 kV, the distance between the needle tip

and the collector was 125 mm, and the pump flow rate was set to 0.5 mL h^{-1} .

Aligned fibers were produced using an original method of collection as described elsewhere.^[30]

3.2. Fibers Morphology and Alignment

The fibers were coated with a conductive layer of sputtered gold and viewed on SEM (JeolJSM-5410) at 15 kV. FFT outputs were used to characterize fibers orientation (ImageJ with Oval profile plug-in).

3.3. Preparation of Biocompatible Hydrogel O-rings

Biocompatible hydrogel O-rings, designed to fit to the wells of 24 well tissue culture plates (Nunc, Denmark), were produced according to a well-established protocol^[45–47] and sterilized by gamma radiation (25 kGy) before the cell culturing experiments. In the course of experiments this study had to introduce an additional 1 mm incision at the rear of O-rings designed to fit

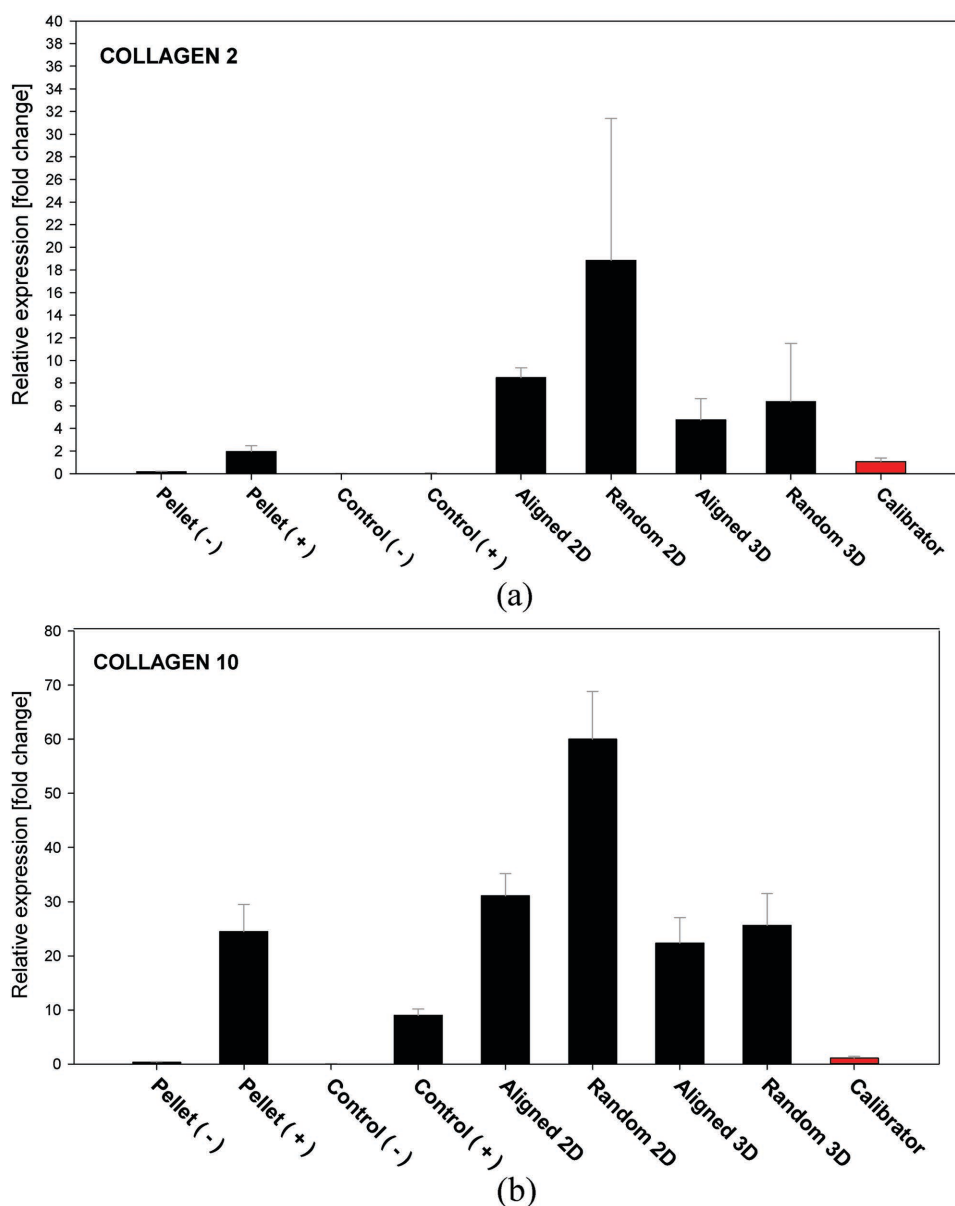


Figure 11. Quantitative RT-PCR for a) Collagen 2 and b) Collagen 10 genes activity of different samples at 50th d of culture. The samples include: control pellets propagated in complete chondrogenic medium (Pellet +), or in basal medium (Pellet –). Additional controls include samples of ADSCs cultured as indicated in (+) or (–) chondrogenic medium in regular tissue culture plates. Experimental samples include the activity of cells cultured as indicated on random and aligned nanofibers in either 2D or 3D configuration.

to an additional holder made from stainless steel wire (Figure 3) intended to fix the direction of aligned fibers deposition (see above), to make easier processing the constructs and to avoid twisting the sample during culture.

3.4. Cells

Human (ADSCs of passage 1 were obtained as frozen samples from Lonza BioWhittaker (Verviers, Belgium) and maintained in DMEM/F12 medium containing 1% GlutaMAX, 1% antibiotic-antimycotic solution and 10% fetal bovine serum (FBS)—all provided from Gibco at 37 °C, 5% CO₂ and 98% humidity. The

medium was replaced each 2nd d until the cells reach ≈90% confluence to be used for the experiments.

3.5. Preparation of 2D and 3D Constructs

Early passage human ADSCs (up to 3rd passage) were harvested with Trypsin/EDTA and seeded onto gel-supported nanofibers scaffolds at density of 2×10^4 cells per sample. The cell-loaded samples were and further cultured for 3–5 d in incomplete chondrogenic medium DMEM supplemented with 10% FBS and 10×10^{-9} M dexamethasone upon rich confluency before being

switched to chondrogenic differentiation conditions under 2D or 3D environment (see Figure 1.3).

For differentiation of cells in 2D environment, the constructs were just switched to complete chondrogenic medium consisting of DMEM supplemented with 10% FBS, TGF β 3 (10 ng mL⁻¹), BMP-6 (10 ng mL⁻¹), and ascorbic acid (5 μ g mL⁻¹) and cultured for 50 d (Figure 1.4). Conversely, for the creation of 3D environment a sandwich-like constructs were assembled via joining two cell-loaded samples facing each other with their cellular site (see Figure 3.3) taking special care to put aligned samples in the same direction using special stainless steel holder fitted to a 1 mm incision at the rear of O-rings was used (see Figure 3.3 providing also easier samples processing).

3.6. Overall Cell Morphology and Cartilage Tissue Visualization

To study the overall cell morphology upon initial contact with nanofibers 2D samples were placed in 24-well TC plates (Nunc, Denmark) and seeded with 5×10^4 cells/well in serum-free medium for 2 h. Actin cytoskeleton was viewed with FITC-Phalloidin (Invitrogen) and focal adhesions were contra stained with monoclonal anti-vinculin antibody (Sigma, Spain) followed by goat anti-mouse AlexaFluor 555-conjugated secondary antibody (Invitrogen, Cat. No. A21428), while cell nuclei were stained by Hoechst (Sigma-Aldrich, Spain). The samples were viewed in an inverted fluorescent microscope (Axio Observer Z1, ZEISS). To confirm cell viability, the samples were stained with FDA (Sigma) at final concentration of 0.001% (W/V) in DMEM and representative pictures were taken at low magnification (10 \times), (see Figure 5).

To measure and compare the thickness of the resulting cartilage, the samples were fixed and cut at the region of the middle hole using biopsy puncher in order to obtain samples from nanofibers layer only. The small tissue disks were cryopreserved using a sucrose gradient before being frozen and cut into a 10 μ m tangential slices that were mounted on microscopic slides and studied under phase contrast.

To follow the distribution of cells, some of the cartilage discs (2D samples only) were stained with FITC-Phalloidin and Hoechst (to view the actin and nuclei) and mounted as above. Comparative Z stack images and optical reconstructions were carried out with Leica TCL-SL confocal microscope and IMARIS software.

3.7. Collagen II Immunofluorescence and Alcian Blue Staining

After fixation with PF 4% for 30 min, both 2D and 3D constructs were cryopreserved using a sucrose gradient. Subsequently, the whole constructs were embedded in optimal cutting temperature compound and cut transversally in 30 μ m slices. Only slices at the gel-free region (consisting only of nanofibers) were collected and placed onto gelatinized glass slides. For immunostaining, slices were washed three times for 5 min in PBS and then blocked for non-specific binding sites by incubation with bovine serum albumin 5% in PBS (PBS-BSA 5%) for 30 min. Primary antibody (monoclonal anti-collagen II; Abcam, ab3092) was diluted 1:100 in PBS-BSA 1%. After 1 h of incubation at 37 °C, slices were then washed in PBS and incubated with the secondary antibody (Alexa

■ Table 1. TaqMan probes.

Target gene	Gene symbol	Assay ID
Collagen 2	COLL2A1	Hs00264051_m1
Collagen 10	COLL10A1	Hs00166657_m1
β -Actin (housekeeping)	ACTB	Hs01060665_g1

Fluor 488 anti-mouse; 1:300, Thermo Scientific; A21151) diluted in PBS-BSA 1% for 1 h at room temperature. Slices received two 5-min washes with PBS and were then incubated with DAPI (DNA intercalation; blue) for 10 min at room temperature. After two more washes with PBS and one with distilled water, slices were mounted in *n*-propyl gallate in 80% glycerol (Sigma-Aldrich) and stored at 4 °C, protected from light. Negative controls were obtained by omitting the primary antibody. Samples were visualized using a Leica TCS SP5 confocal laser scanning microscope. Confocal images were obtained using HCX PL APO 60 \times objective for oil immersion and had a numerical aperture of 1.4. Alternatively, slices were colorized using Alcian Blue dye to detect glycosaminoglycans. Slices were incubated with 1% Alcian Blue solution, pH 2.5 (in 3% acetic acid) for 5 min and washed in distilled water. Brightfield images were obtained using a Nikon Ti microscope.

3.8. Quantitative Real Time PCR

Total cellular RNA was extracted from the middle tissue discs by using RNeasy Mini Kit (QIAGEN, Germany). Reverse transcription was performed by processing of 10 μ L of three times diluted RNA-eluate with High Capacity cDNA Reverse Transcription Kit (Applied Biosystems) according to the suppliers protocol. Quantitative PCR analysis of the gene expression was carried out with fast real-time PCR System (Applied Biosystems 7900HT). Briefly, a single qPCR reaction consisted of mixing 10 μ L Taqman Gene Expression Master Mix (Applied Biosystems), 1 μ L TaqMan primers (Applied Biosystems), 5 μ L nuclease-free H₂O and 4 μ L of sample cDNA. Some details related to TaqMan primers used for the detection of collagen 2 (Col 2), collagen 10 (Col 10), SOX 9 and β -Actin are listed in Table 1. Each sample was run in triplicate and the cycling program was set on 95 °C for 10 min, followed by 40 cycles of 95 °C for 15 s, and 60 °C for 1 min. Data analysis was performed by DataAssist Software (Thermo Fisher Scientific, Spain). Comparative C_T analysis was used to determine the relative expression of each target gene. The amount of the target gene was normalized to β -Actin as housekeeping gene. Transcription levels were expressed as fold change from the calibrator control value (non-activated hADSCs) for each sample.

3.9. Statistical Analysis

Data from all quantitative analysis were expressed as mean \pm standard deviation and subjected to one-way ANOVA variance analysis. Each experiment was performed in triplicates and repeated at least two times. Statistical significance was determined by Student's *t*-test using non-stimulated confluent hADSCs cultures as a control. Probability values with *p* < 0.05 were considered as statistically significant.

Acknowledgements: This work was supported by CIBER-BBN Spain (project BIOSURFACES), and the European Commission through the FP7 Industry-Academia Partnerships and Pathways (IAPP) project FIBROGELNET. The valuable support of the project MAT 2015-69315-C3 MYOHEAL, funded by Spanish Ministry of Science and Innovation is also acknowledged.

Received: March 9, 2016; Revised: May 2, 2016; Published online: ;
DOI: 10.1002/mabi.201600080

Keywords: cartilage; chondrogenic response; collagen; FBG/PLA nanofibers; mesenchymal stem cells

- [1] T. J. Klein, J. Malda, L. Robert, R. L. Sah, D. W. Hutmacher, *Tissue Eng. Part B* **2009**, *15*, 2.
- [2] J. M. McPherson, R. Tubo, *Principles of Tissue Engineering*, 2nd ed. (Eds: R. P. Lanza, R. Langer, J. Vacanti), Academic Pr., San Diego **2000**, pp. 697–771.
- [3] A. R. Poole, *J. Bone Joint Surg.* **2005**, *87*, 1.
- [4] R. J. Daher, N. O. Chahine, A. S. Greenberg, N. A. Sgaglione, D. A. Grande, *Nat. Rev. Rheumatol.* **2009**, *5*, 599.
- [5] A. Bedi, B. T. Feeley, R. J. Williams 3rd, *J. Bone Joint Surg. Am.* **2010**, *92*, 994.
- [6] S. Kim, *Arthritis Rheum* **2008**, *59*, 481.
- [7] J. P. Benthien, M. Schwaninger, P. Behrens, *Knee Surg. Sports Traumatol. Arthrosc.* **2011**, *19*, 543.
- [8] G. Portocarrero, G. Collins, T. Livingston Arinze, *J. Tissue Sci. Eng.* **2013**, *4*, 1.
- [9] R. L. Sah, *The Many Faces of Osteoarthritis* (Eds: K. E. Kuettner, V. C. Hascall), Raven Press, New York **2002**, p. 409.
- [10] R. J. Wade, I. A. Burdick, *Mater. Today* **2012**, *15*, 454.
- [11] E. A. Makris, A. H. Gomoll, K. N. Malizos, J. C. Hu, K. A. Athanasiou, *Nat. Rev. Rheumatol.* **2015**, *11*, 21.
- [12] C. Y. Xu, R. Inai, M. Kotraki, S. Ramakrishna, *Biomaterials* **2004**, *25*, 877.
- [13] Y. Zhang, F. Yang, K. Liu, H. Shen, Y. Zhu, W. Zhang, W. Liu, S. Wang, Y. Cao, G. Zhou, *Biomaterials* **2012**, *33*, 2926.
- [14] J. Qu, D. Zhou, X. Xu, F. Zhang, L. He, R. Ye, Z. Zhu, B. Zuo, H. Zhang, *Appl. Surf. Sci.* **2012**, *261*.
- [15] F. Yang, R. Murugan, S. Wang, S. Ramakrishna, *Biomaterials* **2005**, *26*, 2603.
- [16] C. H. Lee, H. J. Shin, I. H. Cho, Y. M. Kang, I. A. Kim, K. D. Park, J. W. Shin, *Biomaterials* **2005**, *26*, 1261.
- [17] S. Jia, L. Liu, W. Pan, G. Meng, C. Duan, L. Zhang, Z. Xiong, J. Liu, *J. Biosci. Bioeng.* **2012**, *113*, 647.
- [18] R. L. Dahlin, F. K. Kasper, A. G. Mikos, *Tissue Eng. Part B Rev.* **2011**, *17*, 349.
- [19] a) Z. Xiong, J. Liu, *J. Biosci. Bioeng.* **2012**, *113*, 647; b) *Tissue Eng. Part A* **2014**, *14*, 1.
- [20] Y. Cao, J. P. Vacanti, K. T. Paige, J. Upton, C. A. Vacanti, *Plast. Reconstr. Surg.* **1997**, *100*, 297.
- [21] C. A. Vacanti, R. Langer, B. Schloo, J. P. Vacanti, *Plast. Reconstr. Surg.* **1991**, *88*, 753.
- [22] M. Schnabel, S. Marlovits, G. Eckhoff, I. Fichtel, L. Gotzen, V. Vécsei, J. Schlegel, *Osteoarthritis Cartilage* **2002**, *10*, 62.
- [23] S. P. Bruder, D. Gazit, L. Passi-Even, I. Bab, A. I. Caplan, *Bone Miner. Res.* **1990**, *11*, 141.
- [24] J. M. Coburn, M. Gibson, S. Monagleb, Z. Patterson, J. H. Elisseeff, *PNAS* **2012**, *109*, 25.
- [25] J. L. Dragoo, B. Samimi, M. Zhu, S. L. Hame, B. J. Thomas, J. R. Lieberman, M. H. Hedrick, P. Benhaim, *J. Bone Joint Surg. Br.* **2003**, *85-B*, 740.
- [26] P. A. Zuk, M. Zhu, H. Mizuno, et al., *Tissue Eng.* **2001**, *7*, 211.
- [27] D. Gugutkov, J. Gustavsson, M. P. Ginebra, G. Altankov, *Biomater. Sci.* **2013**, *1*, 1065.
- [28] G. E. Wnek, M. E. Carr, D. G. Simpson, G. L. Bowlin, *Nano Lett.* **2003**, *3*, 213.
- [29] S. R. Perumcherry, K. P. Chennazhi, S. V. Nair, D. Menon, A. B. Tech, *Tissue Eng. Part C* **2011**, *17*, 1.
- [30] He Ch, X. Xi, F. Zhang, L. Cao, W. Feng, H. Wang, X. Mo, *J. Biomed. Mater. Res. A* **2011**, *97A*, 339.
- [31] M. Théry, A. Pépin, E. Dressaire, Y. Chen, M. Bornens, *Cell Motil. Cytoskeleton* **2006**, *63*, 341.
- [32] F. Grinnell, *Trends Cell Biol.* **2003**, *13*, 264.
- [33] S. Chandrasekhar, G. W. Laurie, F. B. Cannon, G. E. Martin, H. K. Kleinman, *Proc. Natl. Acad. Sci. USA* **1986**, *83*, 5126.
- [34] M. Sancho-Tello, F. Forriol, P. Gastaldi, A. Ruiz-Sauri, J. J. Martín de Llano, E. Novella-Maestre, C. M. Antolinos-Turpín, J. A. Gómez-Tejedor, J. L. Gómez Ribelles, C. Carda, *Int. J. Artif. Organs* **2015**, *38*, 210.
- [35] Z. Zhang, J. M. McCaffery, R. G. S. Spencer, C. A. Francomano, *J. Anat.* **2004**, *205*, 229.
- [36] H. Muir, D. Bullough, A. Maroudas, *J. Bone J. Surg. Br.* **1970**, *52*, 554.
- [37] J. S. Temenhoff, A. G. Nikos, *Biomaterials* **2000**, *21*, 431.
- [38] A. R. Poole, T. Kojima, T. Yasyuda, F. Mwake, M. Lavwerty, S. Kobayashi, *Clin. Orthop. Relat. Res.* **2001**, *399*.
- [39] J. K. Wise, A. L. Yarin, C. M. Magaridis, M. Cho, *Tissue Eng. Part A* **2009**, *15*, 913.
- [40] W.-J. Li, K. G. Danielson, P. G. Alexander, R. S. Tuan, *J. Biomed. Mater. Res. A* **2003**, *67*, 1105.
- [41] W.-J. Li, Y. J. Jiang, R. S. Tuan, *Tissue Eng.* **2006**, *12*, 1775.
- [42] P. K. Gupta, A. K. Das, A. Chullikana, S. B. Majumdar, *Stem Cell Res. Ther.* **2012**, *3*, 25.
- [43] J. K. Mouw, G. Ou, V. M. Weaver, *Nat. Rev. Mol. Cell Biol.* **2014**, *15*, 771.
- [44] V. C. Hascall, *Biology of Carbohydrates* (Ed: V. Ginsburg), Wiley, New York **1981**, Vol. 1, pp. 1–49.
- [45] A. J. Campillo-Fernandez, M. Salmeron Sanchez, R. Sabater i Serra, J. M. Meseguer Duenas, M. Monleon Pradas, J. L. Gomez Ribelles, *Eur. Polym. J.* **2008**, *44*, 1996.
- [46] D. Gugutkov, C. Gonzalez-Garcia, G. Altankov, M. Salmeron-Sanchez, *J. Bioactive Compatible Polym.* **2011**, *26*, 375.
- [47] N. M. Coelho, C. Gonzalez-Garcia, M. Salmeron-Sanchez, G. Altankov, *Tissue Eng. Part A* **2011**, *17*, 2245.